Syntheses, Structures, and Magnetic Properties of Copper(II) Complexes with 1,3-[Bis(2-pyridylmethyl)amino]benzene (1,3-tpbd) as Ligand

Simon P. Foxon,[a] Gemma Romualdo Torres,[a] Olaf Walter,[b] Jens Zacho Pedersen,[c] Hans Toftlund,[c] Martina Hüber,[d] Karsten Falk,[d] Wolfgang Haase,[d] Joan Cano,[e] Francesc Lloret,[e] Miguel Julve,*[e] and Siegfried Schindler*[a]

Keywords: Copper / Magnetic properties / EPR spectroscopy / Spin polarisation / Dinuclear complexes

The dinuclear copper(II) complexes $\{[Cu_2(1,3\text{-tpbd})(H_2O)(OAc)_2](ClO_4)_2\}_{0.23}\{[Cu_2(1,3\text{-tpbd})(H_2O)_2(OAc)](ClO_4)_3\}_{0.77}\cdot 0.77H_2O$ (**1**), $[Cu_2(1,3\text{-tpbd})(H_2O)_2(OAc)_2](ClO_4)_2\cdot 2H_2O$ (**2**), and the tetranuclear copper(II) complex $[Cu_4(1,3\text{-tpbd})_2(H_2O)_2(SO_4)_4]\cdot 8H_2O$ (**3**) {1,3-tpbd = 1,3-bis[bis(2-pyridylmethyl)amino]benzene} were synthesised and structurally characterised by X-ray diffraction. Variable-temperature (2.0–290 K) magnetic susceptibility measurements on these complexes as well as on the dinuclear copper(II) complex $[Cu_2(1,3\text{-tpbd})(H_2O)_2(ClO_4)_3]ClO_4$ (**4**) (whose structure was published earlier) were performed. In contrast to **2** and **3**, significant ferromagnetic coupling with $J = +9.3$ cm^{-1} was observed for **4** (the Hamiltonian being defined as $\hat{H} = -J\,\hat{S}_1\cdot\hat{S}_2$). Density functional theory (DFT) calculations were used successfully for the interpretation of the ferromagnetic coupling observed in **4**.

Introduction

Continuing interest in the synthesis and characterisation of polynuclear copper(II) complexes derives from the efforts to understand the factors that are responsible for the magnetic exchange interactions between coupled metal centres. Attention has been focused on the magnetostructural correlations and the exchange mechanism involving different bridging groups.[1−7]

The symmetry and energy of the SOMOs ("magnetic orbitals": the molecular orbitals which define each unpaired electron of a paramagnetic centre) and the molecular orbitals of the bridging ligands are important for the understanding of the magnetic exchange phenomena in polynuclear complexes.[3,8−10] The most common situation for magnetic coupling through extended bridges is the antiferromagnetic interaction: the larger the overlap integral between the SOMOs involved, the larger the antiferromagnetic coupling. However, ferromagnetic coupling is observed when the interacting SOMOs are orthogonal to one another: the larger the overlap density between orthogonal SOMOs, the larger the ferromagnetic coupling. Orthogonality can be achieved by either geometrical or topological symmetry; geometrical symmetry has been successfully applied to bimetallic compounds[3] and metal−radical systems.[11] Topological symmetry is being used extensively in designing high-spin organic polyradical species; the intramolecular spin alignment can be explained in terms of the spin polarisation mechanism.[12,13] This mechanism describes how an unpaired electron on one atom polarizes the electron cloud on the adjacent atom in the opposite sense.

Although the spin polarisation mechanism was shown to be valid for some oxygen or nitrogen perturbed systems[14,15] as well as for some organic radical-paramagnetic transition metal ion type systems,[16] the limits of its application are unclear, especially for coordination compounds containing transition metal ions as the only spin sources. In fact, polymeric transition metal complexes containing pyrimidine bridges have been designed as an approach to molecule-based ferromagnets.[17−22] Ward and co-workers provided examples of antiferromagnetic/ferromagnetic coupling between transition metal ions connected by conjugated bridges with an even/odd number of atoms.[19,20]

[a] Institut für Anorganische und Analytische Chemie, Justus-Liebig-Universität Gießen,
Heinrich-Buff-Ring 58, 35392 Gießen, Germany
Fax: (internat.) +49-641-9934-149
E-mail: Siegfried.Schindler@anorg.chemie.uni-giessen.de
[b] Forschungszentrum Karlsruhe, ITC-CPV,
Postfach 3640, 76021 Karlsruhe, Germany
[c] Department of Chemistry, Odense University,
Campusvej 55, 5230 Odense M, Denmark
[d] Institute for Physical Chemistry, Technical University of Darmstadt,
Petersenstraße 20, 64287 Darmstadt, Germany
[e] Department de Química Inorgànica, Facultat de Química, Universitat de València,
Dr. Moliner 50, 46100 Burjassot, València, Spain
Fax: (internat.) +34-96-3544-322
E-mail: miguel.julve@uv.es

Some of us have investigated dinuclear copper complexes with ligands derived from 1,3-phenylenediamine which can be regarded as model compounds for copper proteins.[23,24] However, only a few ligands are described in the literature that are based on a 1,3-phenylenediamine unit.[21,25−30]

We have synthesised and characterised dinuclear copper(I) and copper(II) complexes with the ligand 1,3-bis[bis(2-pyridylmethyl)amino]benzene (1,3-tpbd).[23] A schematic representation of the cation of the copper(II) complex $[Cu_2(1,3\text{-tpbd})(H_2O)_2(ClO_4)_3]ClO_4$ characterised by single-crystal X-ray diffraction is shown below in Figure 1.

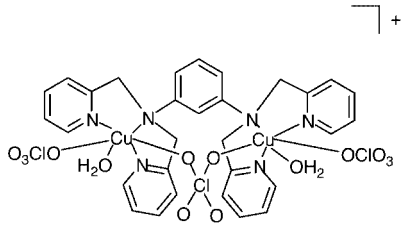

Figure 1. Schematic representation of the molecular structure of the cation of $[Cu_2(1,3\text{-tpbd})(H_2O)_2(ClO_4)_3]ClO_4$ (**4**)

To investigate the effect of substituting the perchlorate bridge in $[Cu_2(1,3\text{-tpbd})(H_2O)_2(ClO_4)_3]ClO_4$ with other anions we synthesised and structurally characterised the dinuclear copper(II) complexes $\{[Cu_2(1,3\text{-tpbd})(H_2O)(OAc)_2](ClO_4)_2\}_{0.23}\{[Cu_2(1,3\text{-tpbd})(H_2O)_2(OAc)](ClO_4)_3\}_{0.77}\cdot 0.77H_2O$ (**1**), $[Cu_2(1,3\text{-tpbd})(H_2O)_2(OAc)_2](ClO_4)_2\cdot 2H_2O$ (**2**), and the tetranuclear copper(II) complex $[Cu_4(1,3\text{-tpbd})_2(H_2O)_2(SO_4)_4]\cdot 8H_2O$ (**3**) and furthermore investigated their magnetic behaviour in comparison with $[Cu_2(1,3\text{-tpbd})(H_2O)_2(ClO_4)_3]ClO_4$ (**4**).

Results and Discussion

Synthesis and Crystal Structures

$[Cu_2(1,3\text{-tpbd})(H_2O)_2(ClO_4)_3](ClO_4)$ (**4**) was prepared and characterised as described previously.[23] Dinuclear cop-

Table 1. Selected bond lengths and bond angles with standard deviations in parentheses for **1a/1b**, **2** and **3**

1a/1b					
Cu(1)−N(1)	2.049(3)	Cu(1)−N(2)	1.951(3)	Cu(1)−N(3)	1.943(3)
Cu(1)−O(2)	1.944(2)	Cu(2)−N(4)	2.100(3)	Cu(2)−N(5)	1.973(3)
Cu(2)−N(6)	1.966(3)	Cu(2)−O(3)	2.215(3)	Cu(2)−O(4)	2.020(3)
O(1)···H(31)	1.81	O(3)−H(31)	0.91		
N(1)−Cu(1)−N(2)	84.51(11)	N(1)−Cu(1)−N(3)	85.05(11)	N(2)−Cu(1)−N(3)	158.73(12)
N(1)−Cu(1)−O(2)	166.91(11)	N(2)−Cu(1)−O(2)	98.29(11)	N(3)−Cu(1)−O(2)	96.06(11)
N(4)−Cu(2)−N(5)	82.68(12)	N(4)−Cu(2)−N(6)	83.38(12)	N(5)−Cu(2)−N(6)	163.70(13)
N(4)−Cu(2)−O(3)	106.24(13)	N(5)−Cu(2)−O(3)	99.40(12)	N(6)−Cu(2)−O(3)	92.58(13)
N(4)−Cu(2)−O(4)	161.12(13)	N(5)−Cu(2)−O(4)	96.71(13)	N(6)−Cu(2)−O(4)	93.75(13)
O(3)−Cu(2)−O(4)	92.51(15)	O(1)···H(31)−O(3)	173.3		
2					
Cu(1)−N(1)	2.067(2)	Cu(1)−N(2)	1.983(2)	Cu(1)−N(3)	1.986(2)
Cu(1)−O(1)	1.999(2)	Cu(1)−O(5)	2.330(2)	Cu(2)−N(4)	2.108(2)
Cu(2)−N(5)	1.969(2)	Cu(2)−N(6)	1.972(2)	Cu(2)−O(3)	1.983(2)
Cu(2)−O(6)	2.194(2)				
N(1)−Cu(1)−N(2)	83.12(9)	N(1)−Cu(1)−N(3)	84.15(9)	N(2)−Cu(1)−N(3)	165.07(10)
N(1)−Cu(1)−O(1)	164.87(9)	N(2)−Cu(1)−O(1)	96.14(9)	N(3)−Cu(1)−O(1)	98.18(9)
N(1)−Cu(1)−O(5)	98.10(9)	N(2)−Cu(1)−O(5)	88.18(9)	N(3)−Cu(1)−O(5)	85.92(9)
N(4)−Cu(2)−N(5)	83.35(9)	N(4)−Cu(2)−N(6)	83.20(9)	N(5)−Cu(2)−N(6)	163.18(9)
N(4)−Cu(2)−O(3)	162.13(8)	N(5)−Cu(2)−O(3)	96.62(9)	N(6)−Cu(2)−O(3)	93.11(9)
3					
Cu(1)−N(1)	2.062(3)	Cu(1)−N(2)	2.032(3)	Cu(1)−N(3)	2.003(3)
Cu(1)−O(1)	1.953(2)	Cu(1)−O(5)	2.159(3)	Cu(2)−N(4)	2.038(3)
Cu(2)−N(5)	2.001(3)	Cu(2)−N(6)	1.986(3)	Cu(2)−N(6)	1.986(3)
Cu(2)−O(6)	1.963(2)	Cu(2)−O(6)#1	2.398(2)	S(1)−O(1)	1.510(2)
S(1)−O(2)	1.469(2)	S(1)−O(3)	1.469(2)	S(1)−O(4)	1.456(2)
S(2)−O(6)	1.528(2	S(2)−O(7)	1.459(3)	S(2)−O(8)	1.462(2)
S(2)−O(9)	1.464(2)	Cu(2)···Cu(2a)	3.316		
N(1)−Cu(1)−N(2)	81.86(10)	N(1)−Cu(1)−N(3)	81.52(11)	N(2)−Cu(1)−N(3)	163.34(11)
N(1)−Cu(1)−O(1)	162.48(10)	N(1)−Cu(1)−O(5)	103.93(12)	N(2)−Cu(1)−O(1)	103.86(10)
N(2)−Cu(1)−O(5)	90.58(11)	N(3)−Cu(1)−O(1)	91.71(11)	N(3)−Cu(1)−O(5)	94.63(11)
O(1)−Cu(1)−O(5)	92.66(11)	N(4)−Cu(2)−N(5)	83.16(11)	N(4)−Cu(2)−N(6)	82.88(11)
N(5)−Cu(2)−N(6)	165.44(11)	N(4)−Cu(2)−O(6)	177.28(10)	N(4)−Cu(2)−O(6)#1	95.90(9)
N(5)−Cu(2)−O(6)	98.03(10)	N(5)−Cu(2)−O(6)#1	98.79(9)	N(6)−Cu(2)−O(6)	96.09(10)
N(6)−Cu(2)−O(6)#1	86.77(9)	O(6)−Cu(2)−O(6)#1	81.51(9)		

Table 2. Crystal data and structure refinement parameters for **1a/1b**, **2** and **3**

Complex	$(\mathbf{1a})_{0.23}(\mathbf{1b})_{0.77}\cdot 0.77H_2O$	**2**	**3**
Empirical formula	$C_{32.44}H_{33.67}Cl_{2.78}Cu_2N_6O_{16.11}$	$C_{34}H_{42}Cl_2Cu_2N_6O_{16}$	$C_{60}H_{76}Cu_4N_{12}O_{26}S_4$
Molecular mass	990.93	988.72	1763.72
Temperature /K	293(2)	293(2)	200(2)
Crystal system	monoclinic	monoclinic	monoclinic
Space group	$P2_1/c$ (No. 14)	$P2_1/n$ (No. 14)	$P2_1/n$ (No. 14)
a (Å)	23.6166(1)	16.995(3)	11.8974(3)
b (Å)	10.0463(2)	12.594(3)	10.7422(2)
c (Å)	17.2188(3)	20.046(4)	27.9871(6)
β /°	102.0280(10)	109.702(17)	101.9850(10)
V (Å^3)	3995.63(11)	4039.5(14)	3498.90(13)
Z	4	4	2
$D_{calcd.}$ /g·cm^{-3}	1.647	1.626	1.674
μ/mm^{-1}	1.329	1.265	1.410
F(000)	2018	2032	1816
Crystal size (mm^3)	0.30 × 0.30 × 0.30	0.20 × 0.20 × 0.25	0.25 × 0.20 × 0.10
θ range for data collection	1.76 to 28.32	1.93 to 28.29	1.49 to 28.30
Index ranges	$-31 \le h \le 31$	$-22 \le h \le 22$	$-15 \le h \le 15$
	$-13 \le k \le 13$	$-16 \le k \le 16$	$-14 \le k \le 13$
	$-22 \le l \le 22$	$-26 \le l \le 26$	$-36 \le l \le 37$
Reflections measured	40879	41742	35485
Unique reflections, R_{int}	9818, 0.0552	9895, 0.0500	8516, 0.0815
Completeness to θmax	93.3%	94.4%	93.1%
Data/restraints/parameters	9818/0/620	9895/0/641	8516/0/527
Goodness of fit on F^2	1.016	0.999	0.999
Final R indices	$R1 = 0.0498$	$R1 = 0.0429$	$R1 = 0.0471$
$[I > 2\sigma(I)]$	$wR2 = 0.1258$	$wR2 = 0.0972$	$wR2 = 0.0801$
R indices (all data)	$R1 = 0.0933$	$R1 = 0.0812$	$R1 = 0.0996$
	$wR2 = 0.1454$	$wR2 = 0.1125$	$wR2 = 0.0968$
Max./min. electron density /e·Å^{-3}	+0.929/−0.939	+1.287/−0.809	+0.519/−0.489

per(II) complexes with acetate or sulfate as additional anionic ligands in place of perchlorate were obtained by mixing the appropriate copper(II) salts with 1,3-tpbd in methanol/water mixtures.

Acetate can display varying modes of coordination in its copper(II) complexes: bridging, bidentate and monodentate coordination modes of this ligand are well-known and for the sake of brevity only a few examples are given in the cited references.[31−37] Our first attempt of reacting together 1,3-tpbd, copper(II) perchlorate and copper(II) acetate resulted in a mixture of blue and green crystals. The molecular structure of both compounds was solved by single-crystal X-ray diffraction; the blue crystals showed disorder at one copper(II) ion indicating that in the unit cell there were two different complexes present, denoted **1a** and **1b**, which were found in a 23 to 77 ratio respectively. The contents of the unit cell can be represented as $\{[Cu_2(1,3\text{-tpbd})(H_2O)(OAc)_2](ClO_4)_2\}_{0.23}\{[Cu_2(1,3\text{-tpbd})(H_2O)_2(OAc)](ClO_4)_3\}_{0.77}\cdot 0.77H_2O$ ($\mathbf{1a}_{0.23}\mathbf{1b}_{0.77}\cdot 0.77H_2O$). In **1a** the copper(II) ion Cu(1) is tetra-coordinated to three N-donor atoms of the 1,3-tpbd ligand and one O atom of an acetate, the ligands forming a distorted square planar environment around the copper(II) ion (Figure 2 and Table 1 and 2). The coordination geometry around the copper(II) ion Cu(2) is square pyramidal; Cu(2) is bound to three N-donor atoms of the 1,3-tpbd ligand, one O atom of an acetate ion [O(4) in Figure 2] and one O-donor atom of a coordinated water molecule.

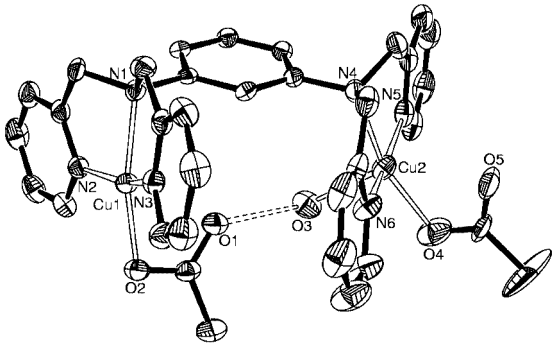

Figure 2. ORTEP representation (30% probability displacement ellipsoids) of the cation of **1a** (hydrogen atoms are omitted for clarity)

The copper(II) coordination environments in **1a** and **1b** differ; one of the coordinated acetate anions in **1a** [O(4) in Figure 2] is replaced by a water solvent molecule and an additional perchlorate anion is found in the unit cell.

An intramolecular hydrogen bond formed by the water solvent molecule O(3), which is always coordinated to Cu(2), and the non-coordinated O atom O(1) of the acetate ligand bound to the other copper ion Cu(1) leads to further stabilisation (Table 2).

The dark green crystals were characterised as $[Cu_2(1,3\text{-tpbd})(H_2O)_2(OAc)_2](ClO_4)_2\cdot 2H_2O$ (**2**) and the molecular

structure of the cation of **2** is shown in Figure 3 (Table 1 and 2). Each copper(II) centre is five-coordinate and their coordination geometries are best described as square pyramidal.

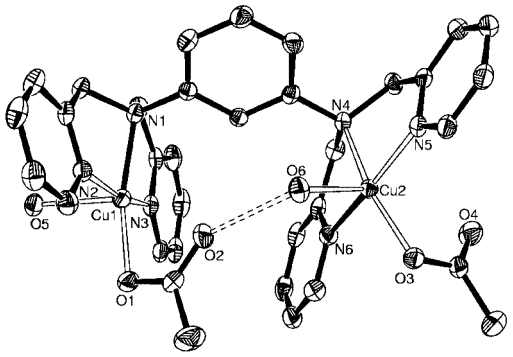

Figure 3. ORTEP representation (30% probability displacement ellipsoids) of the cation of **2** (hydrogen atoms are omitted for clarity)

2 was obtained in a pure form by mixing 1,3-tpbd and copper(II) acetate stoichiometrically (1:2) in methanol/water with an excess of sodium perchlorate. Only large green crystals of **2** were grown from that solution. An excess of acetate ions in solution is necessary to avoid substitution of the acetate ligands by water molecules.

In contrast to **4**, where a perchlorate ion bridges the two copper(II) ions in the solid state, the acetate ions in **1a**, **1b** and **2** coordinate only in a monodentate fashion. The Cu−O bond lengths in **1a**, **1b** and **2** (Table 2) are similar to those found in other monodentate acetate-containing copper(II) complexes and the $Cu-N_{pyridine}$ bonds are shorter than the $Cu-N_{amine}$ bonds.[35,37] In the cases where the copper(II) ion is coordinated by an axial ligand, the bond lengths of Cu−O are clearly longer than those in the equatorial positions. Bond lengths and angles of **1** and **2** compare well with **4**. The Cu···Cu distances in **1** (6.06 Å) and **2** (5.85 Å) are similar to **4** (5.87 Å)[23] even though the two copper(II) ions are not bridged by acetate.

Sulfate was also chosen to replace the perchlorate bridge in **4**. There are numerous examples of structurally characterised transition metal complexes with sulfate as a bridging ligand (a limited number of examples are given in the references).[38−43] Mixing stoichiometric amounts of copper(II) sulfate and 1,3-tpbd (2:1) in water lead to the formation of dark blue crystals after slow evaporation at room temperature. The molecular structure revealed that the tetranuclear complex $[Cu_4(1,3\text{-tpbd})_2(H_2O)_2(SO_4)_4]\cdot 8H_2O$ (**3**) formed (Figure 4 and Table 1 and 2) with the sulfate ion acting as both a terminal ligand and as a bridging ligand.

Each copper(II) ion in **3** is five-coordinate and their coordination geometries are best described as distorted square pyramidal. The two sulfate-bridged copper(II) ions are separated by 3.316 Å. The sulfate anions exhibit an unusual one atom bridging mode which is reflected in the different S−O bond lengths of 1.515(2) Å (coordinated oxygen) and 1.461(2) Å (mean value, uncoordinated oxygens). The Cu···Cu distances through the bridging 1,3-tpbd units (7.20 Å) in **3** are much longer than in **1**, **2** or **4**. We are aware of only one other example of a bis-sulfate bridged copper(II) complex $[Cu(HL)(SO_4)]_2$ (HL = 2-formylpyridine thiosemicarbazone) which has been structurally characterised.[39] The geometry of the coordination sphere around the copper(II) ions in $[Cu(HL)(SO_4)]_2$ is distorted square-pyramidal, with bond lengths and angles for $[Cu(HL)(SO_4)]_2$ similar to those observed in **3**.

Magnetic Properties of 2, 3 and 4

The temperature dependence of $\chi_M T$ for **4** (χ_M is the magnetic susceptibility per two copper(II) ions) is shown in Figure 5.

At room temperature, $\chi_M T$ is equal to 0.85 $cm^3\cdot K\cdot mol^{-1}$, the expected value for two magnetically isolated spin doublets. Upon cooling, the value of $\chi_M T$ increases, attaining a maximum at 3.5 K and then decreasing slightly further. This behaviour is typical of a ferromagnetically coupled dinuclear copper(II) complex, the small decrease of $\chi_M T$ in the low temperature range being due to weak intermolecular magnetic interactions.

The susceptibility data of **4** were analysed through a simple Bleaney−Bowers expression[44] for two magnetically interacting local spin doublets derived from the Hamiltonian $\hat{H} = -J\,\hat{S}_1\cdot\hat{S}_2$ ($\hat{S}_1 = \hat{S}_2 = 1/2$) with the inclusion of a θ parameter to account for the intermolecular interactions. Least-squares best-fit results are: $J = +9.3\ cm^{-1}$, $g = 2.12$, $\theta = -0.08$ K and $R = 1.8 \times 10^{-6}$ (R is the agreement factor defined as $\Sigma_i[(\chi_M T)_{obsd.}(i) - (\chi_M T)_{calcd.}(i)]^2/$

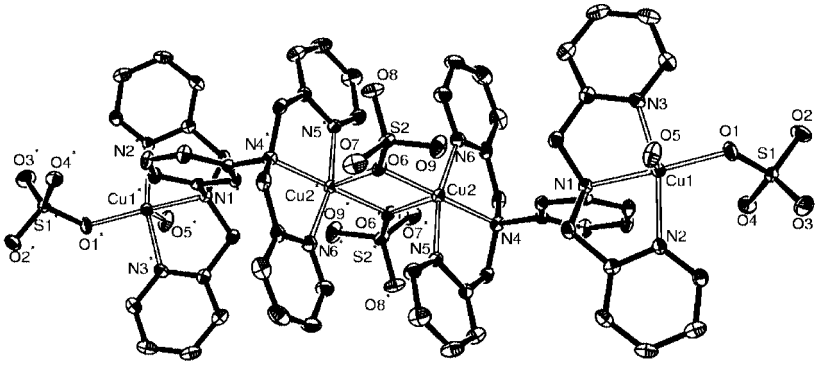

Figure 4. ORTEP representation (30% probability displacement ellipsoids) of **3** (hydrogen atoms are omitted for clarity)

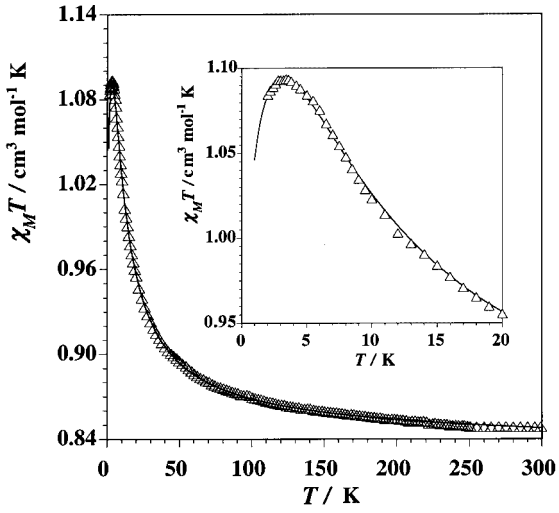

Figure 5. Thermal variation of $\chi_M T$ for **4**: (△) experimental data; (−) best fit (see text). The inset shows the maximum of $\chi_M T$ in the low-temperature region (applied magnetic field of 0.1 T)

$\Sigma_i[(\chi_M T)_{obsd.}(i)]^2$). The theoretical curve (solid line in Figure 5) fits the experimental data well as indicated by the low value of the agreement factor. The magnetisation versus H plot up to 5 T (maximum available magnetic field with our SQUID) at 2 K (Figure 6) tends to a saturation value of ca. 2.1 BM as expected for a $S = 1$ spin state with $g = 2.12$.

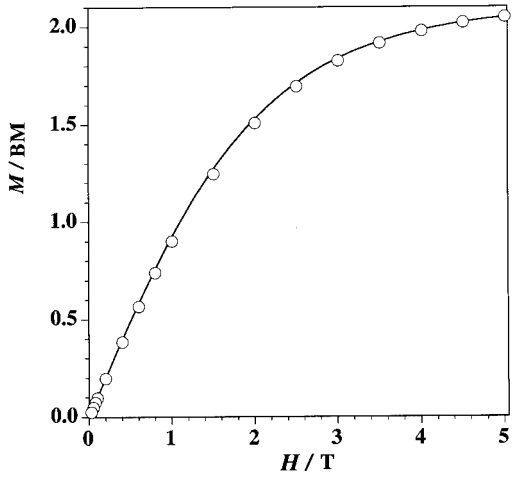

Figure 6. M versus H plot at 2 K for **4**: (o) experimental data; (–) Brillouin function for an $S = 1$ spin state with $g = 2.12$

The EPR spectrum of **4** in methanol (Figure 7) was recorded at X-band frequency at 100 K to elucidate further the nature of the magnetic coupling. The spectrum shows a seven line splitting pattern in the $g_{||}$ region, with the 1:2:3:4:3:2:1 intensity pattern characteristic of a coupled dinuclear Cu^{II} system. A similar signal, but with much lower intensity, due to the forbidden $\Delta M = \pm 2$ state was observed around 1500 G. The observed half-field signal confirms the presence of a $Cu^{II}-Cu^{II}$ triplet state. No changes in the positions of the signals were observed in this spectrum when working at 5 K.

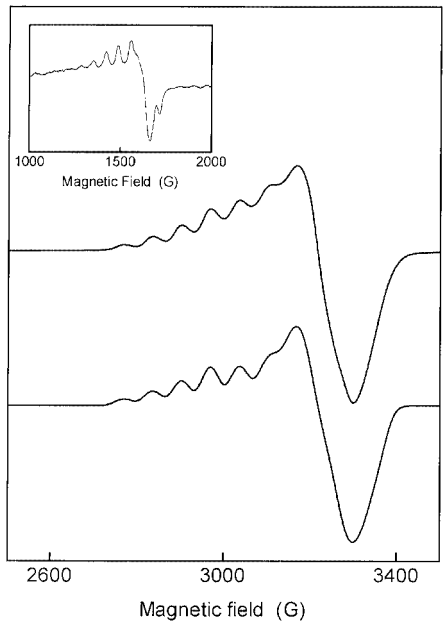

Figure 7. Top: Measured EPR spectrum of **4** in methanol/water; Bottom: Simulated spectrum. The inset shows the measured EPR spectrum at half-field

Magnetic susceptibility measurements of **2** were problematic. A large crystal, which was taken out of the mother liquor, was investigated immediately and no magnetic coupling could be detected during the magnetic measurements. This behaviour changed when the crystal became dry with a ferromagnetic coupling of ca. $J = +9.1$ cm^{-1} observed. Ferromagnetic coupling was observed when smaller crystals were used which seemed to loose water molecules when a vacuum was applied during the magnetic measurements. Most likely, carboxylate-assisted water loss occurs and the structural change associated with this process [carboxylate bridge between Cu(1) and Cu(2)] would lead to a 1,3-tbpd-bridged dicopper(II) fragment very close in nature to that observed for **4**, the magnetic coupling of the anhydrous phase of **2** being essentially identical to that of **4**.

EPR measurements of **2** were unsuccessful in providing a complete description of the magnetic behaviour. The EPR spectrum of the pure green crystals dissolved in methanol demonstrated that at least a mixture of three species exists under these conditions. This is similar to our findings during the structural characterisation of the complexes, where from one solution three different complexes were obtained. Clear changes in the EPR spectra were observed by adding sodium perchlorate or sodium acetate indicating the presence of equilibria in solution. Even though no "clean" EPR spectrum could be measured for **2**, we observed that no triplet state at half field was detected under the same conditions as for **4**, in agreement with the magnetic susceptibility measurements of the large crystal. Therefore, it is clear that none of the acetate complexes in methanolic solutions [most likely species consisting of differing amounts of acetate and water molecules coordinated to the copper(II)

ions as shown in Figure 2 and 3] provide a magnetic exchange pathway for ferromagnetic coupling.

Magnetic susceptibility measurements of **3** failed to provide any information that magnetic coupling between the copper(II) ions in this complex takes place. **3** showed typical normal magnetic behaviour of four magnetically isolated copper(II) ions and the data followed a Curie law. This finding is the same as the findings obtained for $[Cu(HL)(SO_4)]_2$ where no magnetic exchange phenomena were detected.[39] EPR spectra of **3** could not be obtained because the complex is insoluble in methanol and those performed in water or methanol/water mixtures were not well resolved.

The number of ferromagnetically coupled dinuclear copper(II) complexes is small when compared to that of antiferromagnetically coupled ones.[1,3,32,34,45–52] Herein, different bridging groups were found to provide a magnetic exchange pathway for ferromagnetic coupling in dinuclear copper(II) complexes. However, in all these cases (with the exception of a related complex reported recently[21]) the distance between the two copper(II) ions is much less than 5.87 Å as in **4**. Moreover, magnetic exchange coupling over large distances is often weak and antiferromagnetic.[3,6,53,54]

Examining the structure of **4** (Figure 1), two possible exchange pathways could be operative, one involving the phenylenediamine unit and the other involving the perchlorate bridge. The latter pathway is ruled out taking into account that the perchlorate oxygen is axially coordinated to the copper(II) ion [2.39 Å for Cu–O(perchlorate)].[23] As the unpaired electron of the copper(II) ion is delocalised only in the four short equatorial bonds, it is clear that the spin density on the perchlorate oxygen should be very small. A similar conclusion was reached by Murray and coworkers for the perchlorate bridged complex $[Cu_2L^1(ClO_4)_2]\cdot 2H_2O$ [L^1 = *N*-(2-pyridinyl)acetoacetamide].[55] Furthermore, from the X-ray structure data of **4** the intermolecular exchange interaction can be excluded: the shortest intermolecular copper–copper distance is 8.67 Å, with no ligand present which could provide a possible exchange pathway. Consequently, the exchange pathway involved in the ferromagnetic coupling observed in **4** is operating through the *meta*-phenylenediamine bridge. In contrast to **4**, complexes with either a *para*-phenylenediamine (pd) bridge as in $[(tren)Cu(pd)Cu(tren)]^{4+}$[56,57] [tren = tris(2-aminoethyl)amine], or the dinuclear copper(II) complex of the *para* homologue of 1,3-tpbd, $[Cu_2(1,4\text{-tpbd})(H_2O)_4](S_2O_6)_2$ ($J = -15.56$ cm^{-1}),[58] show weak antiferromagnetic coupling.

The relatively weak exchange coupling of the unpaired electrons of the copper(II) ions in **4** is expected since the superexchange pathway, attributed to magnetic exchange coupling interactions, is most often described as operating via the sigma bond framework. In the case of $[Cu_2(1,4\text{-tpbd})(H_2O)_4](S_2O_6)_2$ the pathway is seven bonds long. A comparison of the magnetic coupling observed in $[Cu_2(1,4\text{-tpbd})(H_2O)_4](S_2O_6)_2$ with the magnetic coupling observed in **4** provides a demonstration of the spin-polarisation mechanism between paramagnetic ions via an aromatic organic bridging group. Ferromagnetism is predicted in cases where there is an odd number of bridging atoms and antiferromagnetic exchange coupling with an even number of bridging atoms. With five atoms between the copper(II) ions in **4**, the σ framework is one bond shorter than that in $[Cu_2(1,4\text{-tpbd})(H_2O)_4](S_2O_6)_2$. The two SOMOs involved in **4** are almost perpendicular to the phenyl ring and the unpaired electrons in the $d_{x^2-y^2}$ orbitals of both copper(II) ions can interact via this pathway. Thus the nature of the exchange coupling observed in these two complexes (ferro- in **4** and antiferromagnetic in $[Cu_2(1,4\text{-tpbd})(H_2O)_4](S_2O_6)_2$] is expected using this model.

In order to interpret the ferromagnetic interaction present in **4**, DFT calculations were performed (see paragraph of Computational Methodology in the Exp. Sect.)[23] on the model systems depicted in Figure 8 (**I**–**IV**), where the donor nitrogen atoms of 1,3-tpbd have been replaced by ammonia molecules (model **IV** corresponds to the complex **4**).

In the four models, the unpaired electron on each copper(II) ion (that is the SOMO) lies in the basal plane of the

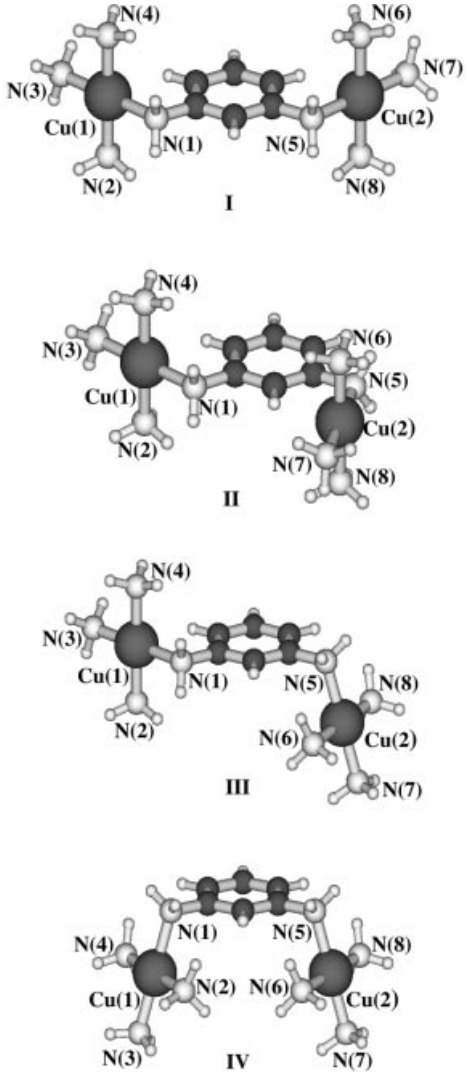

Figure 8. Model systems (**I**–**IV**) of dinuclear copper(II) complexes which were used to carry out the DFT type calculations (see text)

metal ion [comprising of atoms N(1), N(2), N(3), and N(4) for Cu(1) and N(5), N(6), N(7), and N(8) for Cu(2)]. The orientation of the two SOMOs with respect to the phenylenediamine plane is gradually varied in **I**−**IV** in such a manner that the exchange interaction is transmitted through either pure σ (**I** and **II**) or π (**IV**) pathways, whereas **III** is a mixed σ-π type. The calculated values of *J* for models **I**−**IV** are −1.7, −0.1, +0.6 and +7 cm^{-1}, respectively.

The analysis of the trend for the observed *J* values shows that the magnetic interaction is weak and antiferromagnetic in **I** and **II**, with that of **I** being somewhat larger. The SOMOs in these models are perpendicular to the plane of the phenylenediamine plane, but they differ in their conformation: *anti-anti* in **I** versus *anti-syn* in **II**. The σ in-plane overlap between the SOMOs of Cu(1) and Cu(2), through the long pathway Cu(1)−N(1)−C−C−C−N(5)−Cu(2) in both models, is expected to be weak and poorer in the case of **II** because of its *anti-syn* configuration. Since the antiferromagnetic interaction in a dinuclear copper(II) complex is proportional to the square of the overlap integral between the SOMOs,[56,57] the value of the antiferromagnetic coupling in **I** and **II** is expected to be very small and weaker for **II**. In the case of **III** the SOMO of Cu(2) lies below the plane of the phenylenediamine plane, whereas that of Cu(1) remains unchanged. In this situation, although the set of atoms involved in the exchange pathway is the same as in **I** and **II** [Cu(1)−N(1)−C−C−C−N(5)−Cu(2)], the spin density on N(1) is of a σ type whereas that on N(5) is of a π type. Consequently, a zero overlap between the SOMOs will result (case of accidental orthogonality) and a ferromagnetic coupling interaction is expected. This coupling has to be small because of the extended bridging pathway involved.[56,57] In the case of model **IV** the two SOMOs, being perpendicular to the phenylenediamine plane, lie below this plane. The spin density on the N(1) and N(5) amine nitrogens is of the π type. The DFT calculations for this model indicate a ground triplet spin state lying below the excited singlet spin state. The calculated value of *J* for **IV** (+7 cm^{-1}) agrees well with the experimental value obtained for **4** from the fit of the susceptibility data ($J = +9.3\ cm^{-1}$). To qualitatively understand this result, a focus on the nature of the singly occupied molecular orbitals (SOMOs) depicted in Figure 9 (a) is helpful.

The SOMOs are composed of the in-phase and out-of-phase combinations of the 3d orbitals of the copper(II) ions with two π-type nonbonding molecular orbitals of appropriate symmetry of the *meta*-phenylenediamine unit. In these SOMOs there is an antibonding interaction between the $d_{x^2-y^2}$ orbital of the copper(II) ion and the p_z atomic orbital of the nitrogen atoms of the bridging ligand. This interaction involves: i) an energy gap between the two SOMOs following the rules formulated by Kanamori and Goodenough or Kahn's model.[3,8−10] Since the orbitals of the ligands involved in the building of these SOMOs are of a non-bonding character and, consequently, similar energies, and since the electronic densities on the nitrogen atoms are also similar in both orbitals, the two resultant SOMOs

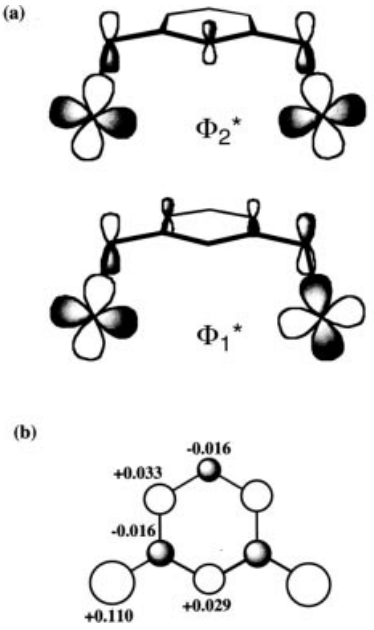

Figure 9. Schematic representation of (a) the two SOMOs and (b) the spin density distribution on the bridge region for **4** on the basis of DFT calculations. Empty and full contours represent positive and negative spin densities, respectively. Calculated average atomic spin densities are presented

(φ_1* and φ_2*) are practically degenerate, with a small energy gap of 347 cm^{-1}; ii) a spin delocalisation from the copper(II) ion to the nitrogen atom of the π system of the bridging skeleton, that accounts for the transmission of the exchange. Thus, the direct overlap between the $d_{x^2-y^2}$ orbital of the metal ion and the π system of the pyridyl ligand allows the unpaired spin of the metal to induce a polarisation of spin on the bridging skeleton (see Figure 9), as occurs in similar compounds described by Ung et al.[20] These systems constitute very interesting cases because of the strong competition between spin delocalisation and spin polarisation, prevailing the alternating spin rule in our case, as shown by experimental data and theoretical calculations.

Conclusion

Complex **4** is an example of a dinuclear copper(II) complex showing ferromagnetic exchange coupling over quite a long distance. The ferromagnetic coupling in **4** is due to the non-coplanarity of the metal coordination planes, leading to a folded structure, placing the two SOMOs in **4** practically perpendicular to the phenyl ring. The symmetry in **4** breaks down if the bridging perchlorate ion is substituted by a non-bridging acetate ion as in **2** and the magnetic interaction vanishes. The magnetic coupling in the dehydrated phase of **2** is essentially identical to that of **4**. Such a fact suggests that the carboxylate-assisted loss of the coordinated water molecule in **2** leads to a carboxylato-bridged species where the carboxylato group mimics the perchlorato group in **4**, leading to a very similar structure. The relative arrangement of the SOMOs of the copper(II) ions, with re-

spect to the *meta*-phenylenediamine plane, and the fact that the sulfate-oxygen occupies an equatorial position of one copper(II) ion [Cu(2A)] and the axial one at the adjacent copper(II) ion [Cu(2)] account for the lack of magnetic coupling in the tetrameric complex **3**.

Experimental Section

General Remarks: Reagents and solvents used were of commercially available reagent grade quality. 1,3-tpbd and **4** were synthesised as described previously.[23] Electron spin resonance measurements at X-band frequency were obtained using a Bruker EMX-113 spectrometer. Samples in methanol or methanol water (9:1) mixtures were measured at 100 K. Simulation of all EPR spectra was made with the Bruker SimFonia program. Magnetic susceptibility data were collected: a) Over the temperature range 4.2−295 K at an applied magnetic field of 0.56−1.5 T. The measurements were performed using a Faraday-type magnetic balance, equipped with a Cahn D-200 microbalance and a Bruker B-MN 200/60 electromagnet.[59] The sample constituted of microcrystals contained in a quartz basket which was calibrated independently, using $HgCo(SCN)_4$ as calibrant. The diamagnetic correction of the magnetic susceptibility was calculated using Pascal's constants. b) Over the temperature range 2.0−290 K with a Quantum Design SQUID susceptometer and using an applied magnetic field of 0.1 T (compounds **2** and **4**). The susceptometer was calibrated with $(NH_4)_2Mn(SO_4)_2{\cdot}12H_2O$.

Computational Methods: The computational strategy used in the present work has been fully described elsewhere,[60] and it is briefly outlined here. For the evaluation of the coupling constant for each model compound (**I**−**IV**, Figure 8), two separate calculations were carried out using DFT, one for the triplet state and another one for the low-spin, broken symmetry state. The hybrid B3LYP method[61] was been used in the calculations as implemented in GAUSSIAN 98,[61] with all-electron double-ζ basis proposed by Ahlrichs and co-workers except for copper where we have used a triple-ζ basis.[62] Ammonia molecules were used as peripheral ligands in **I**−**IV** and the bond lengths and angles are those of the average values of the real structures. The complete dimeric structures were used in the calculations to estimate the values of *J*.

Caution! *Perchlorate salts are potentially explosive and should be handled with great care. Our preparations were carried out on mmol scale and heating was avoided.*

Mixture of $[Cu_2(1,3\text{-tpbd})(H_2O)(OAc)_2](ClO_4)_2$/$[Cu_2(1,3\text{-tpbd})(H_2O)_2(OAc)](ClO_4)_3$ (1a/1b) and $[Cu_2(1,3\text{-tpbd})(H_2O)_2(OAc)_2](ClO_4)_2$ (2): To a suspension of 1,3-tpbd (250 mg, 0.5 mmol) in methanol (15 mL) was added a solution of $Cu(ClO_4)_2{\cdot}6H_2O$ (195 mg, 0.525 mmol) and $Cu(OAc)_2{\cdot}H_2O$ (104 mg, 0.525 mmol) in water (20 mL). The green solution was stirred for a few minutes, filtered and crystals suitable for X-ray analysis formed after a few days.

$[Cu_2(1,3\text{-tpbd})(H_2O)_2(OAc)_2](ClO_4)_2{\cdot}2H_2O$ (2): To a suspension of 1,3-tpbd (250 mg, 0.5 mmol) in methanol (15 mL) was added a solution of $Cu(OAc)_2{\cdot}H_2O$ (208 mg, 1.05 mmol) in 20 mL of water. After an excess of solid $NaClO_4$ was added to the green solution it was stirred for a few minutes, filtered and left on the shelf. Crystals suitable for X-ray analysis formed after a few days. Yield 267 mg (54%). $C_{34}H_{42}Cl_2Cu_2N_6O_{16}$ (988.7): calcd. C 41.30, H 4.28, N 8.50; found C 40.94, H 4.06, N 8.48.

$[Cu_4(1,3\text{-tpbd})_2(H_2O)_2(SO_4)_4]{\cdot}8H_2O$ (3): To a suspension of 1,3-tpbd (300 mg, 0.63 mmol) in methanol (15 mL) was added a solution of $Cu(SO_4)_2{\cdot}6H_2O$ (315 mg, 1.26 mmol) in water (20 mL). The deep green solution was stirred for a few minutes, filtered and blue crystals suitable for X-ray analysis formed after a few days. Yield 220 mg (40%). $C_{60}H_{76}Cu_4N_{12}O_{26}S_4$ (1763.7): calcd. C 40.86, H 4.34, N 9.53; found C 40.86, H 4.58, N 9.40.

X-ray Crystallographic Study: Crystal data and experimental conditions are listed in Table 2. The molecular structures are illustrated in Figures 2−4. Selected bond lengths and bond angles with standard deviations in parentheses are presented in Table 1. Intensity data were collected on a Siemens SMART 5000 CCD-Diffractometer with graphite monochromated Mo-K_α radiation (λ = 0.71073 Å). The collected reflections were corrected for Lorentz, polarisation and absorption effects.[63] The structures were solved by direct methods and refined by full-matrix-least-squares methods on F^2.[64,65] CCDC-204112, -204113, and -204114 contain the supplementary crystallographic data for this paper. These data can be obtained free of charge at www.ccdc.cam.ac.uk/conts/retrieving.html [or from the Cambridge Crystallographic Data Centre, 12 Union Road, Cambridge CB2 1EZ, UK; Fax: (internat.) + 44-1223/336-033; E-mail: deposit@ccdc.cam.ac.uk].

Acknowledgments

S. S. and W. H. gratefully acknowledge financial support from the Volkswagen-Stiftung and the Deutsche Forschungsgemeinschaft. Furthermore, we thank Dr. Achim Elvers and Prof. Dr. Ulrich Zenneck (University of Erlangen-Nürnberg) for their assistance with the first EPR measurements and helpful discussions. S. S. furthermore thanks Prof. Dr. Rudi van Eldik (University of Erlangen-Nürnberg) for his support of this work. Financial support from the Spanish Ministry of Science and Technology through Project BQ2001−2928 is also acknowledged.

[1] O. Kahn, *Comments, Inorg. Chem.* **1984**, *3*, 105.
[2] O. Kahn, *Angew. Chem. Int. Ed. Engl.* **1985**, *24*, 834.
[3] O. Kahn, *Molecular Magnetism*, Wiley-VCH, Weinheim, **1993**.
[4] M. Kato, Y. Muto, *Coord. Chem. Rev.* **1988**, *92*, 45.
[5] W. E. Hatfield, *Comments, Inorg. Chem.* **1981**, *1*, 105.
[6] K.-S. Bürger, P. Chaudhuri, K. Wieghardt, B. Nuber, *Chem. Eur. J.* **1995**, *1*, 583.
[7] R. D. Willet, D. Gatteschi, O. Kahn, *Magneto-Structural Correlations in Exchange Systems*; Reidel, Dordrecht, **1985**.
[8] J. B. Goodenough, *Phys. Rev.* **1955**, *100*, 654.
[9] J. Kanamori, *J. Phys. Chem. Solids* **1959**, *10*, 87.
[10] P. W. Anderson, *Solid State Phys.* **1963**, *14*, 99.
[11] A. Caneschi, D. Gatteschi, R. Sessoli, *Acc. Chem. Res.* **1989**, *22*, 392.
[12] H. M. McConnell, *J. Chem. Phys.* **1963**, *39*, 1910.
[13] N. Mataga, *Theor. Chim. Acta* **1968**, *10*, 372.
[14] F. Kanno, K. Inoue, N. Koga, H. Iwamura, *J. Phys. Chem.* **1993**, *97*, 13267.
[15] M. Kitano, Y. Ishimaru, K. Inouw, N. Koga, H. Iwamura, *Inorg. Chem.* **1994**, *33*, 6012.
[16] N. Koga, H. Ishimanu, H. Iwamara, *Angew. Chem. Int. Ed. Engl.* **1996**, *108*, 815.
[17] T. Ishida, T. Nogami, *Recent Res. Dev. Pure Appl. Chem.* **1997**, *1*, 1.
[18] H. Oshio, *J. Chem. Soc., Chem. Commun.* **1991**, 240.
[19] A. M. W. C. Thompson, D. Gatteschi, J. A. McCleverty, J. A. Navas, E. Rentschler, M. D. Ward, *Inorg. Chem.* **1996**, *35*, 2701.
[20] V. A. Ung, A. M. W. C. Thompson, D. A. Bardwell, D. Gatteschi, J. C. Jeffery, J. A. McCleverty, F. Totti, M. D. Ward, *Inorg. Chem.* **1997**, *36*, 3447.

[21] I. Fernández, R. Ruiz, J. Faus, M. Julve, F. Lloret, J. Cano, X. Ottenwaelder, Y. Journaux, M. C. Munõz, *Angew. Chem. Int. Ed.* **2001**, *113*, 3129.
[22] T. Glaser, M. Gerenkamp, R. Fröhlich, *Angew. Chem. Int. Ed.* **2002**, *114*, 3984.
[23] S. Schindler, D. J. Szalda, C. Creutz, *Inorg. Chem.* **1992**, *31*, 2255.
[24] S. Schindler, *Eur. J. Inorg. Chem.* **2000**, 2311.
[25] T. N. Sorrell, M. L. Garrity, D. J. Ellis, *Inorg. Chim. Acta* **1989**, *166*, 71.
[26] N. N. Murthy, M. Mahroof-Tahir, K. D. Karlin, *J. Am. Chem. Soc.* **1993**, *115*, 10404.
[27] M. Mahroof-Tahir, N. N. Murthy, K. D. Karlin, N. J. Blackburn, S. N. Shaikh, J. Zubieta, *Inorg. Chem.* **1992**, *31*, 3001.
[28] M. Mahroof-Tahir, K. D. Karlin, *J. Am. Chem. Soc.* **1992**, *114*, 7599.
[29] R. Hernández-Molina, A. Mederos, P. Gili, S. Domínguez, F. Lloret, J. Cano, M. Julve, C. Ruiz-Pérez, X. Solans, *J. Chem. Soc., Dalton Trans.* **1997**, 4327.
[30] S. Domínguez, A. Mederos, P. Gili, A. Rancel, A. E. Rivero, F. Brito, F. Lloret, X. Solans, C. Ruiz-Pérez, M. L. Rodríguez, I. Brito, *Inorg. Chim. Acta* **1997**, *255*, 367.
[31] T. N. Sorrell, C. O′Connor, O. P. Anderson, J. H. Reibenspies, *J. Am. Chem. Soc.* **1985**, *107*, 4199.
[32] V. McKee, M. Zvagulis, J. V. Dagdigian, M. G. Patch, C. A. Reed, *J. Am. Chem. Soc.* **1984**, *106*, 4765.
[33] P. K. Coughlin, S. J. Lippard, *J. Am. Chem. Soc.* **1984**, *106*, 2328.
[34] G. Christou, S. P. Perlepes, E. Libby, K. Folting, J. C. Huffmann, R. J. Webb, D. N. Hendrickson, *Inorg. Chem.* **1990**, *29*, 3657.
[35] M. Vaidyanathan, R. Viswanathan, M. Palaniandavar, T. Balasubramanian, P. Prabhaharan, T. P. Muthiah, *Inorg. Chem.* **1998**, *37*, 6418.
[36] Y. Nishida, M. Takeuchi, K. Takahashi, S. Kida, *Chem. Letters* **1983**, 1815.
[37] J. A. Halfen, W. B. Tolman, *J. Am. Chem. Soc.* **1994**, *116*, 5475.
[38] H. Endres, D. Nothe, E. Rossato, W. E. Hatfield, *Inorg. Chem.* **1984**, *23*, 3467.
[39] A. G. Bingham, H. Bögge, A. Müller, E. W. Ainscough, A. M. Brodie, *J. Chem. J. Chem. Soc., Dalton Trans.* **1987**, 493.
[40] D. A. Buckinham, C. R. Clark, J. Simpson, W. T. Robinson, *Inorg. Chem.* **1988**, *27*, 3544.
[41] K. Wieghardt, S. Drueke, P. Chaudhuri, U. Florke, H.-J. Haupt, B. Nuber, J. Weiss, *Z. Naturforsch., Teil B* **1989**, *44*, 1093.
[42] M. A. de Britto, A. Neves, I. Vencato, C. Zucco, V. Drago, K. Giesar, W. Haase, *J. Braz. Chem. Soc.* **1997**, *8*, 443.
[43] L. K. Thompson, X. Zhiqiang, A. E. Goeta, J. A. K. Howard, H. J. Clase, D. O. Miller, *Inorg. Chem.* **1998**, *37*, 3217.
[44] B. Bleaney, K. Bowers, *Proc. Roy. Soc., Sect. A* **1952**, *214*, 451.
[45] A. M. Greenaway, C. J. O′Connor, J. W. Overman, E. Sinn, *Inorg. Chem.* **1981**, *20*, 1508.
[46] A. K. Gregson, N. T. Moxon, *Inorg. Chem.* **1982**, *21*, 3464.
[47] A. L. van den Brenk, K. A. Byriel, D. P. Fairlie, L. R. Gahan, G. R. Hanson, C. J. Hawkins, A. Jones, C. H. L. Kennard, B. Moubaraki, K. Murray, *Inorg. Chem.* **1994**, *33*, 3549.
[48] Y. Zang, Z. Yin, G. Wang, C. Zeng, A. Dai, Z. Zhou, *Inorg. Chem.* **1990**, *29*, 560.
[49] G. Kolks, S. J. Lippard, J. V. Waszczak, *J. Am. Chem. Soc.* **1980**, *102*, 4832.
[50] J. F. Villa, W. E. Hatfield, *J. Chem. Phys.* **1971**, *55*, 4758.
[51] J. F. Villa, W. E. Hatfield, *Inorg. Chem.* **1971**, *10*, 2038.
[52] P. Illiopoulos, K. S. Murray, R. Robson, J. Wilson, G. A. Williams, *J. Chem. Soc., Dalton Trans.* **1987**, 1585.
[53] R. Veit, J. J. Girerd, O. Kahn, F. Robert, Y. Jeannin, *Inorg. Chem.* **1986**, *25*, 4175.
[54] R. Vicente, J. Ribas, S. Alvarez, A. Segui, X. Solanz, M. Verdaguer, *Inorg. Chem.* **1987**, *26*, 4004.
[55] P. Illiopoulos, G. D. Fallon, K. S. Murray, *J. Chem. Soc., Dalton Trans.* **1986**, 437.
[56] T. R. Felthouse, E. N. Duesler, D. N. Hendrickson, *J. Am. Chem. Soc.* **1978**, *100*, 618.
[57] T. R. Felthouse, D. N. Hendrickson, *J. Am. Chem. Soc.* **1978**, *17*, 2636.
[58] T. Buchen, A. Hazell, L. Jessen, C. J. McKenzie, L. Preuss Nielson, J. Z. Pedersen, D. Schollmeyer, *J. Chem. Soc., Dalton Trans.* **1997**.
[59] S. Gehring, P. Fleischhauer, H. Paulus, W. Haase, *Inorg. Chem.* **1993**, *32*, 54.
[60] E. Ruiz, P. Alemany, S. Alvarez, J. Cano, *J. Am. Chem. Soc.* **1997**, *119*, 1297.
[61] A. D. Becke, *J. Chem. Phys.* **1993**, *98*, 5648.
[62] A. Schaefer, H. Horn, R. Ahlrichs, *J. Chem. Phys.* **1992**, *97*, 2571.
[63] Siemens Area Detector Absorption Correction, Siemens.
[64] G. M. Sheldrick, *SHELX-97*, University of Göttingen, **1997**.
[65] L. Zsolnai, *XPMA*, University of Heidelberg, **1997**.

Received July 1, 2003
Early View Article
Published Online November 4, 2003

